



Flanders
State of
the Art

14_094_5
FHR reports

Modeling long-term morphodynamic evolution of the Scheldt estuary and its mouth area

Effects of secondary tidal basins

DEPARTMENT
MOBILITY &
PUBLIC
WORKS

www.flandershydraulicsresearch.be

Modeling long-term morphodynamic evolution of the Scheldt estuary and its mouth area

Effects of secondary tidal basins

Nnafie, A.; Van Oyen, T.; De Maerschalck, B.; Verwaest, T.; Mostaert, F.

Legal notice

Flanders Hydraulics Research is of the opinion that the information and positions in this report are substantiated by the available data and knowledge at the time of writing.
 The positions taken in this report are those of Flanders Hydraulics Research and do not reflect necessarily the opinion of the Government of Flanders or any of its institutions.
 Flanders Hydraulics Research nor any person or company acting on behalf of Flanders Hydraulics Research is responsible for any loss or damage arising from the use of the information in this report.

Copyright and citation

© The Government of Flanders, Department of Mobility and Public Works, Flanders Hydraulics Research 2017
 D /2017/3241/89

This publication should be cited as follows:

Nnafie, A.; Van Oyen, T.; De Maerschalc, B.; Plancke, Y.; Verwaest, T.; Mostaert, F. (2017). Modeling long-term morphodynamic evolution of the Scheldt estuary and its mouth area: Effects of secondary tidal basins. Version 2.0. FHR Reports, 14_094_5. Flanders Hydraulics Research: Antwerp.

Until the date of release reproduction of and reference to this publication is prohibited except in case explicit and written permission is given by the customer or by Flanders Hydraulics Research. Acknowledging the source correctly is always mandatory.

Document identification

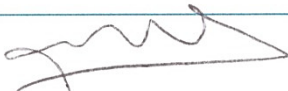
Customer:	Vlaams Nederlands Scheldecommissie (VNSC)	Ref.:	WL2017R14_094_5
Keywords (3-5):	Morphodynamic evolution, secondary basins, estuary, closure, Scheldt, Sloe, Braakman		
Text (p.):	23	Appendices (p.):	/
Confidentiality:	<input checked="" type="checkbox"/> Yes	Released as from:	01/01/2020
		Exception:	<input type="checkbox"/> The Government of Flanders

Author(s):	Nnafie, A.
------------	------------

Control

	Name	Signature
Reviser(s):	Van Oyen, T.; De Maerschalc, B.; Plancke, Y.	
Project leader:	Van Oyen, T	

Approval

Coordinator research group:	Verwaest, T.	
Head of Division:	Mostaert, F.	



Abstract

The specific objective of this study is to investigate impact of the presence of secondary tidal basins on long-term estuarine morphodynamics. To this end, first, a morphodynamic model using Delft3D software is set up, which is able to reproduce large-scale bottom features similar to those observed in real estuaries. Second, runs are conducted with the latter model in case that secondary tidal basins are present. The Scheldt estuary is selected as the study area, where multiple secondary tidal basins were present in the past (e.g. Sloe and Braakman). To compare model results with observations, secondary tidal basins are constructed at the same positions as those of former basins Sloe and Braakman.

In the case of using present geometric shape of the Scheldt estuary (default case), good resemblance between modeled and measured bathymetry is observed, even though significant differences occur. In particular, the simulated formation of a shallow region in the mouth of the estuary flanked by two distinct southern and northern channels, and of a system of straight and meandering channels inside the estuary, are large-scale features that are comparable to observed bathymetry. Moreover, the simulated connection between the main ebb channel in the estuary and the southern channel in the mouth, with the latter extending seaward over time, is confirmed by historical bathymetric data. A significant difference between simulated and measured bathymetries is that the southern channel in the mouth area forms too far south compared with the observed main channel in this area (Wielingen). Another major difference is that many small-scale secondary channels appear in the mouth, which are not observed in the field. Appearance of these small-scale bathymetric features is attributed to neglecting of waves.

Similar to the case of absence of secondary basins (default case), a system of straight flood and meandering ebb channels occurs also in case of presence of the Sloe basin. Main difference is that in the latter case, the part of the ebb channel that is located near this basin forms ~ 2 km more to the south with respect to its location in the default case. These results suggest that the presence of this secondary basin causes a locally southward migration of the ebb channel. Similar southward migration of the ebb channel occurs in case that both Sloe and Braakman basins are present. However, in this case, the meandering ebb channel is wider and the flood channels are less pronounced compared with those in the case of only the Sloe basin. Adding only the Braakman basin weakens the connection between the landward and seaward parts of the ebb channel, which results in a decrease of the sinuosity (meander) of this channel. The presence of Braakman basin does not result in a local displacement of the ebb channel, which reveals the importance of basin location. Results further show that the presence of secondary tidal basins leads to changes in the shape of the meandering ebb channel, such that the connection between the latter channel and the southern channel in the mouth area is weakened, particularly in the case of Braakman basin. This means that the presence of a secondary tidal basin inside the estuary not only have local morphodynamic effects, but it can also have significant impact on the morphodynamic evolution of the mouth of the estuary. This is also confirmed by the fact that sand balance of the entire estuarine system (estuary+mouth) changes significantly in case that secondary basins are added to the system.

Based on the model results, it can be stated that observed northward migration of the ebb channel near the location of former secondary basin Sloe is due to closure of this basin. Moreover, these results suggest that the closure of Sloe and Braakman basins probably have affected to morphological evolution of the Scheldt mouth area.

Contents

Abstract.....	III
List of Figures	VI
List of Tables	VII
Nederlandse samenvatting.....	1
1 Introduction.....	2
2 Study area: Scheldt estuary	4
2.1 Hydrodynamics	4
2.2 Present morphology	4
2.3 Historical morphological development	5
3 Model description	8
3.1 Equations of motion	8
4 Methodology	10
4.1 Experimental set-up.....	10
4.2 Methodology to analyze results	11
5 Model results	12
5.1 Default configuration	12
5.2 Effects of secondary tidal basins.....	15
5.3 Sensitivity to morphological factor	18
6 Discussion and Conclusions	19
References	22

List of Figures

Figure 1	Delft3D computational grid	3
Figure 2	Geometrical shape Scheldt estuary in 1800 AD.....	3
Figure 3	Measured 2011 bathymetry of the Scheldt estuary.....	4
Figure 4	Width-averaged bedlevel of the Scheldt estuary versus the long-channel distance	5
Figure 5	Bathymetric maps of the Western Scheldt and its mouth area between 1804 and 1972	6
Figure 6	Initial bedlevel for different configurations	10
Figure 7	Snapshots of bedlevel at different points in time.....	12
Figure 8	Global growth rate of bedlevel versus time and a comparison between measured and modeled bedlevels	13
Figure 9	Comparison between measured and modeled bedlevels in case of river discharge	14
Figure 10	Comparison between measured and modeled hypsometries	14
Figure 11	Time evolution of the cumulative sand volume changes	15
Figure 12	Time evolution of the cumulative sand volume changes in case of river discharge	15
Figure 13	Modeled bedlevel in case of different model configurations	16
Figure 14	Time evolution of the cumulative sand volume changes in case of Sloe and Braakman.	17
Figure 15	Spatial distribution of bedlevel in case of different morphological amplification factors	18
Figure 16	Obtained bedlevel in case of including waves	21

List of Tables

Table 1	List of model runs.....	11
---------	-------------------------	----

Nederlandse samenvatting

In deze studie wordt de impact van secundaire getijdebekkens op de lange termijn morfologische evolutie van de Westerschelde onderzocht, waarbij gebruik wordt gemaakt van het model Delft3D. Deze getijdebekkens zijn op dezelfde locatie geplaatst als die van de voormalige getijdebekkens in de Westerschelde (Sloe en Braakman). Als eerste stap wordt de gemodelleerde bodem zonder getijdebekken vergeleken met de gemeten bodem, waarbij de focus ligt op de vergelijking van de grootschalige bodemkenmerken. Vervolgens worden de getijdebekkens toegevoegd aan het systeem.

In de situatie zonder getijdebekkens worden in de monding een noordelijke en een zuidelijke geul met daartussen een ondiep gebied gesimuleerd (te vergelijken met Oostgat, Wielingen en Vlake van de Raan). In het estuarium wordt een stelsel van rechte en meanderende geulen uit het model verkregen. Deze grootschalige bodemkenmerken komen goed overeen met de metingen. Een significant verschil tussen modelresultaten en waarnemingen is dat de hoofdgeul “Wielingen” in het model teveel naar het zuiden ligt ten opzichte de werkelijkheid. Een ander belangrijk verschil is dat er teveel nevengeulen in de monding verschijnen die niet voorkomen in de Scheldemonding. Dit laatste heeft te maken met het feit dat golven niet in het model zijn meegenomen.

In de situatie met een enkel getijdebekken op dezelfde locatie als die van Sloe, bevindt de hoofdgeul zich ongeveer 2 km ten zuiden ten opzichte van zijn ligging in het geval zonder getijdebekken. Dit verschil in de ligging van de hoofdgeul nabij het getijdebekken komt ook voor in het geval van het toevoegen van een tweede getijdebekken op dezelfde locatie als die van Braakman. Wel blijkt in het laatste geval dat de hoofdgeul zwakker meandert. Het plaatsten van een enkel getijdebekken op de locatie van Braakman veroorzaakt geen verschuiving van de hoofdgeul, hetgeen betekent dat de locatie van het bekken ook van invloed is. Behalve veranderingen in het estuarium laten modelresultaten zien dat de aanwezigheid van getijdebekkens ook morfologische veranderingen in de monding teweegbrengen. Deze veranderingen worden ook bevestigd door het feit dat de zandbalans van het hele systeem (estuarium + monding) ingrijpend verandert wanneer getijdebekkens worden toegevoegd. Deze model resultaten leveren bewijs dat de waargenomen migratie van de hoofdgeul nabij Sloe over de laatste 200 jaar hoogstwaarschijnlijk het gevolg is van het inpolderen van dit bekken. Bovendien suggereren deze modelresultaten dat het inpolderen van de getijdebekkens in de Westerschelde mogelijk invloed hebben gehad op de morfologische evolutie van de monding.

1 Introduction

Many estuaries are situated in very densely populated areas with high economic activities that often conflict with their ecological values. For centuries, geometry and bathymetry of estuaries have been drastically modified through engineering works, such as embanking, sand extraction, channel deepening, closure of secondary tidal basins, etc. It is generally recognized that these interventions have resulted in significant hydrodynamic and morphological changes in these estuaries (e.g. increasing tidal range and SPM concentrations, loss of intertidal areas, formation of new shoals and channels, channel migration (cf. Peters, 2006; Wang *et al.*, 2009; Winterwerp and Wang, 2013). Examples include the Ems estuary (Germany and The Netherlands), the Loire (France), the Scheldt (Belgium and The Netherlands), the Elbe (Germany) and the Yangtze (China).

Much work has been done to investigate impacts of human interventions on the tidal characteristics and sediment transport in estuaries (e.g. Alebregtse and Swart, 2014; Bolle *et al.*, 2010; Roos and Schuttelaars, 2015; Winterwerp and Wang, 2013). However, knowledge of effects of these interventions on the long-term morphodynamic evolution of estuaries (order decades to centuries) is still lacking. To successfully manage estuarine systems under the ever increasing pressure of population and economic growth, it is therefore necessary to improve our understanding of potential impacts of engineering works on long-term morphodynamic evolution of these systems.

The overall aim of the study is to develop an idealized morphodynamic model that is able to reproduce similar large-scale bottom patterns as those observed in an estuary and its mouth area. The idealized modeling approach is applied as the focus of this study is on improving fundamental understanding of the system. The specific objective of the present work is to investigate impact of the presence of secondary tidal basins on long-term estuarine morphodynamics. To this end, first, a morphodynamic model is developed, which is able to reproduce large-scale bottom features similar to those observed in real estuaries. Second, runs are conducted with the latter model in case that secondary tidal basins are present. The state-of-the-art numerical model Delft3D is used, which has been successfully applied to morphodynamic modeling of estuaries and other coastal systems (cf. Dissanayake *et al.*, 2012; Eelkema *et al.*, 2013; Hibma *et al.*, 2003; Ridderinkhof *et al.*, 2014; Van der Wegen and Roelvink, 2008). Moreover, the current study applies a realistic estuarine geometry, which is based on that of the Scheldt estuary (Fig. 1). Main motivation to consider this estuary is that it used to consist of multiple secondary tidal basins (Sloe, Braakman and Hellegat, see Fig. 2) that were located at different positions in the estuary. These tidal basins have been gradually closed off between 1800 and 1968 (Van der Spek, 1997). Because of the large availability of historical data on geometry and bathymetry of the Scheldt estuary since 1800, a great opportunity to compare model results with observations is provided.

The next chapter describes the hydrodynamic characteristics and the morphological development of the study area. In Chapter 3, a description of the model equations is given. Subsequently, in Chapter 4, the set-up of the model experiments is outlined. Results from these experiments are presented in Chapter 5. Finally, Chapter 6 contains a discussion and the conclusions.

Figure 1 – Delft3D computational grid (red), which covers entire Scheldt estuary and part of the North Sea. Focus area of present study is indicated by white rectangle. The yellow arrow indicates direction of the propagating tidal wave in the North Sea (south-north).

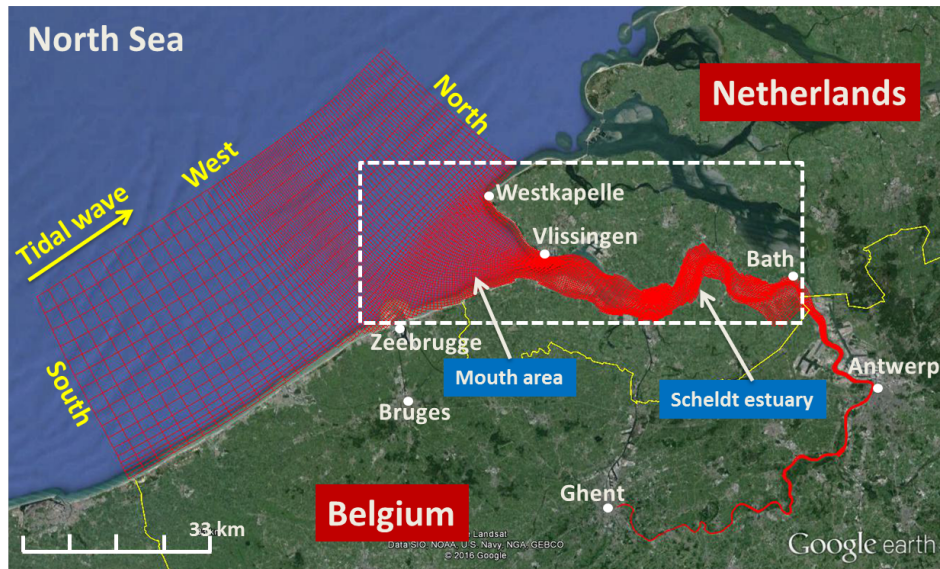


Figure 2 – Geometrical shape Scheldt estuary in 1800 AD. Source: The department Maritime Access, The Government of Flanders.



2 Study area: Scheldt estuary

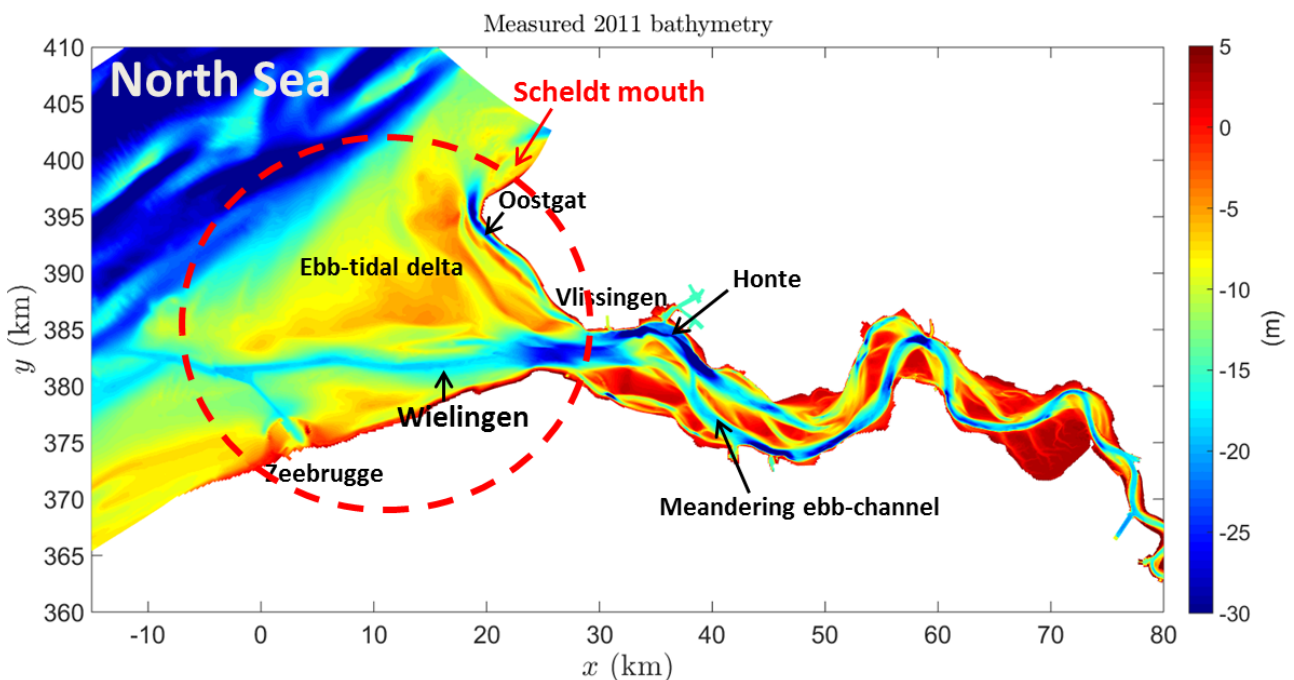
2.1 Hydrodynamics

The Scheldt estuary is a macro-tidal estuary in which the flow field is dominated by (semi-diurnal) tidally induced currents. The river discharge ranges between 50 to 200 m³/s (Van Rijn, 2010), meaning that approximately $\sim 10^6$ m³ of fresh water enters the estuary per semi-diurnal tidal cycle. Given the fact that this discharge is less than 1% of the tidal prism ($\sim 2 \times 10^9$ m³ per semi-diurnal tidal cycle, Wang *et al.*, 2002), the estuary is well-mixed with a constant fluid density over the water depth. The tidal range (difference between high and low water) varies in the range of 2.5 m at neap tide to 4.7 m at spring tide. Moreover, the tidal curve at Westkapelle has a very regular (almost sinusoidal) pattern, whereas further upstream the wave becomes more asymmetric, with a faster tidal rise from low water to high water than otherwise. Furthermore, measurements of the free surface elevation along the estuary show that the tidal range increases in the landward direction up to Rupelmonde (~ 105 km from Westkapelle), after which it decreases further upstream.

2.2 Present morphology

The Scheldt estuary is located in the northwest of Belgium and the southwest of The Netherlands and extends over ~ 175 km from Ghent (Belgium) to Westkapelle (The Netherlands), see Fig. (1). The upper (landward) part of the estuary from Ghent to the Dutch-Belgian border forms the Sea Scheldt.

Figure 3 – Measured 2011 bathymetry (in meters with respect to Mean Sea Level = MSL) of the lower part of the Scheldt estuary. Red circle denotes the Scheldt mouth, which is the transition area between estuary and North Sea.



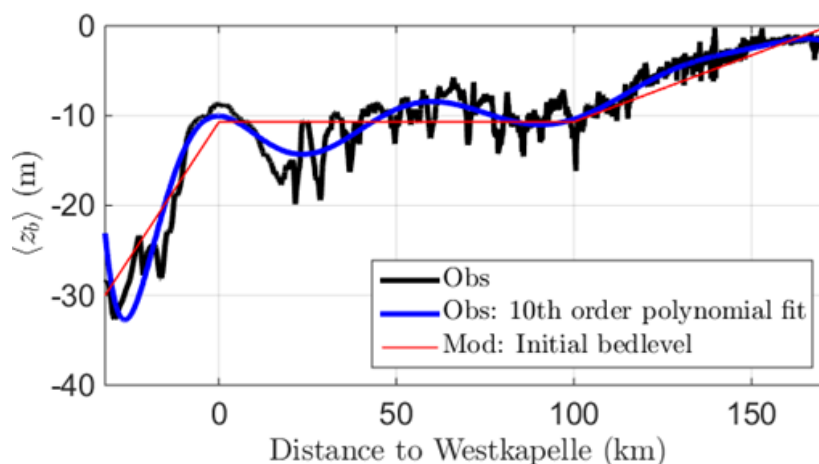
The lower (seaward) part of the estuary, which is the focus of the present study (white rectangle in Fig. 1), consists of the Western Scheldt and its mouth area. The latter area extends seaward from Vlissingen to several kilometers offshore of Westkapelle (denoted by red circle in Fig. 3). The -20m -isobath is generally used to mark the division between the mouth area and the North Sea (Du Four *et al.*, 2006; Slikke M. J., 1999). The Sea Scheldt has a funnel-shaped geometry with an exponentially decreasing width from about $\sim 6\text{ km}$ near the border to $\sim 50\text{ m}$ near Ghent. The width of the lower part of the estuary is roughly constant ($\sim 6\text{ km}$) between the border and upstream of Vlissingen. Further downstream near Vlissingen, width narrows to $\sim 4.6\text{ km}$, which marks the transition between the Western Scheldt and the mouth area. In the latter area, the width strongly increases to $\sim 25\text{ km}$ near Westkapelle.

The bathymetry of Western Scheldt features a multiple channel system, separated by elongated tidal flats (Fig. 3). This channel system is characterized by relative short straight flood channels and meandering ebb channels (Winterwerp *et al.*, 2001). The bathymetry of the Scheldt mouth area is characterized by a sequence of banks with adjacent channels and shallow platforms. The main channels in this area are Oostgat, which occurs along the coast between Vlissingen and Westkapelle, and Wielingen, an ebb-dominated channel at the southern part of the mouth area that is connected with the main ebb channel in the estuary. Channel Wielingen is used as the main shipping route towards various harbors within the estuary (e.g. Sloe, Terneuzen and Antwerp harbors). The bathymetry of the mouth area echoes the characteristics of several morphological features. On the one hand, the shallower region flanked by the Wielingen and Oostgat resembles an ebb-tidal delta; while the sequence of banks and channels in the northern part of the mouth region suggests the presence of elongated tidal sand bars.

2.3 Historical morphological development

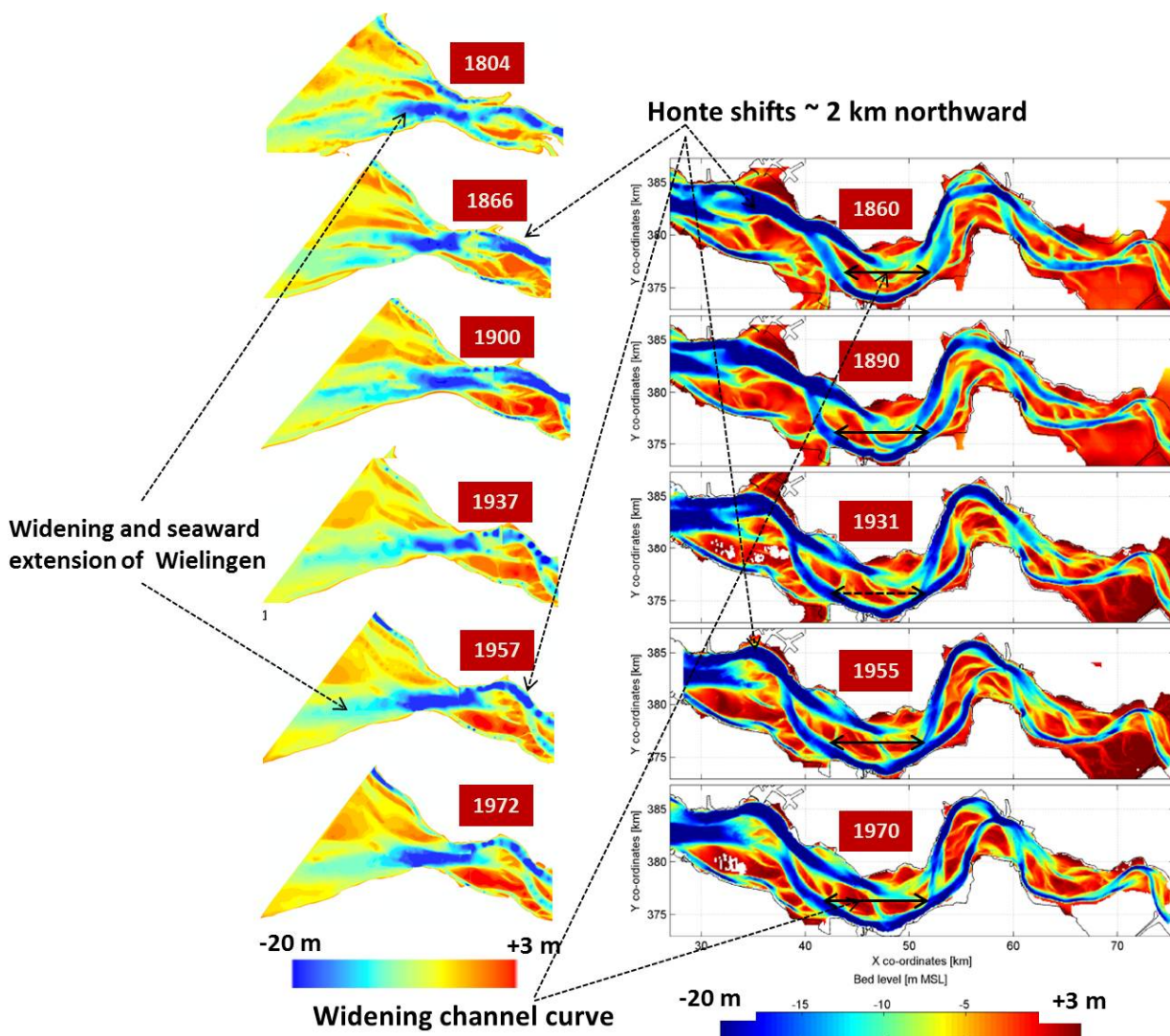
Fig. 5 shows the morphological evolution of the Western Scheldt (right) and its mouth area (left) over the last two centuries. From the left panels several large-scale morphological changes can be observed, among which the widening and seaward extension of channel Wielingen. It is generally thought that the changes in this channel are mainly the result of deepening to increase ship access-

Figure 4 – Width-averaged bedlevel $\langle z_b \rangle$ (black line) of the Scheldt estuary, which is derived from measured bathymetry in 2011, versus the long-channel distance with respect to Westkapelle. The blue line is a 10th order polynomial fit to the observations (blackline) and the red line is the initial bedlevel used in model experiments. Abbreviations "Obs" and "Mod" refer to observed and modeled quantities, respectively.



ibility. However, the left panels of this figure reveal that the latter changes occurred in the beginning of the 20th century, whereas deepening of this channel started much later, viz. in the 1950s. This implies that other factors must have caused the widening and more seaward extension of this channel. Another striking morphological change that can be seen in the left panels of Fig. 5, is a northward rotation of the sequence of banks and channels in the central and northern part of the mouth area. Moreover, the latter area has evolved from a multiple tidal channel system (top left panel) to a system dominated by two main channels (bottom left panel). The morphology of the estuary (right panels in Fig. 5) has also changed significantly since 1860. Numerous secondary channels and shoals appeared and disappeared. The bottom part of the main ebb channel migrated to the outer banks of the estuary and its seaward part (Honte) has shifted by about 2 km northward, thereby increasing its sinuosity (meander). For more details on the historical morphological development of the Scheldt estuary and its mouth area, the reader is referred to e.g. Brand *et al.* (2016), Enckevort (1996), Peters (2006), Peters *et al.* (2001), Slikke M. J. (1999), Spek (1994) and Van Oyen *et al.* (2016).

Figure 5 – Bathymetric maps (in meters with respect to MSL) of the Western Scheldt (right panels) and its mouth area (left panels) between 1804 and 1972. Left and right plots are adopted from the works by Brand *et al.*, 2016 and Dam *et al.*, 2016, respectively. Arrows indicate some large-scale morphological changes in the estuary and mouth area.



The above described morphological changes might be part of the natural morphodynamic evolution of a system that has not yet reached its morphodynamic equilibrium, but they can also be caused by variations in external condition such as increasing tidal amplitude and sea level (Kuijper and Lesinski, 2012; Van den Berg, 1987). As discussed by Peters (2006), the morphological changes in the mouth area can also be attributed to changes in the geometric shape of the Western Scheldt estuary caused by land reclamations and fixation of the alignment of this estuary (Jeuken and Wang, 2010; Spek, 1994; Winterwerp *et al.*, 2001). It is striking to observe the widening of the ebb channel curve (indicated by solid arrows in right panels of Fig. 5) as a result of channel migration towards locations where former secondary basins were present; viz. Braakman and Hellegat. Moreover, the northward shift of the seaward part of this ebb channel (Honte) occurred near the location of former basin Sloe. Considering the correlation in time of closing secondary tidal basins and the observed morphological changes in the estuary, it is hypothesized that the later changes are likely due to closure of these basins. The present work aims at investigating whether this hypothesis hold, by means of the previously introduced numerical model Delft3D.

3 Model description

In this study the Delft3D hydro- and morphodynamic model is used in two-dimensional (depth-averaged) mode (for a detailed description see Lesser *et al.*, 2004). The approach in this study is to apply an idealized model approach by schematizing the tidal forcing (three harmonic constituents M_2 , M_4 and M_6) and initial bathymetry and excluding as many processes as possible (such as waves, winds and sea level rise). Below, equations that govern hydrodynamics, sediment transport and bed level update are presented.

3.1 Equations of motion

The hydrodynamics considered are described by full nonlinear shallow water equations

$$\frac{\partial D}{\partial t} + \vec{\nabla} \cdot (D\vec{v}) = 0, \quad (1)$$

$$\frac{\partial \vec{v}}{\partial t} + \left(\vec{\nabla} \cdot \vec{v} \right) \vec{v} + f \vec{e}_z \times \vec{v} = -g \vec{\nabla} \eta - \frac{g \sqrt{u^2 + v^2}}{C^2 D} \vec{v} + \frac{1}{D} \left(\vec{\nabla} \cdot D\nu \vec{\nabla} \right) \vec{v}. \quad (2)$$

Here, D is the local water depth, \vec{v} is the depth-averaged velocity with components u and v in the cross-channel (x) and long-channel (y) direction, f is the Coriolis parameter, \vec{e}_z is a unit vector in the vertical direction (indicated by the vertical coordinate z), g is the acceleration due to gravity, η is the sea surface elevation with respect to the undisturbed water level ($z = 0$), $\vec{\nabla}$ is the horizontal nabla operator (components $\frac{\partial}{\partial x}$, $\frac{\partial}{\partial y}$), C is the Chézy friction coefficient, ν is the horizontal eddy viscosity, and t is time. Constant values for coefficients C and ν are chosen in both models.

The sediment transport formula applied in this model is Engelund and Hansen, 1967. This formula estimates the total transport vector \vec{Q}_0 (sum of bed load transport and suspended load transport), which is in the direction of \vec{v} , according to:

$$\vec{Q}_0 = \frac{0.05\alpha|v|^4}{\sqrt{g}C^3\delta^2d_{50}} \vec{v}, \quad (3)$$

where α is a calibration coefficient (order 1); $|v| = \sqrt{u^2 + v^2}$ is the magnitude of flow velocity; $\delta = (\rho_s - \rho_w)/\rho_w$ is the relative density with ρ_s and ρ_w the sediment and water densities, respectively; and d_{50} is the median grain size.

Furthermore, to account for bed slope effects, the correction method of Flokstra and Koch, 1981, is applied by multiplying the above sediment transport formula by a factor $1 - \beta \partial z_b / \partial s$, thus:

$$\vec{Q} = \vec{Q}_0 \left(1 - \beta \frac{\partial z_b}{\partial s} \right), \quad (4)$$

with β a bed slope coefficient, s a coordinate in the flow direction and z_b the bed level.

The bed level change is determined by computing the divergence of the total sediment transport,

$$\frac{\partial z_b}{\partial t} = -\frac{1}{1-p} \vec{\nabla} \cdot \vec{Q}, \quad (5)$$

with p is the porosity of the bottom layer, considered constant and equal to 0.4 in the considered analysis.

The morphodynamic time scale is much longer (order years to decades) than the hydrodynamic time scale (order days). This allows for accelerated bed level change by multiplying the time in the above equation by a factor α_{MOR} (Roelvink, 2006).

A combination of water-level boundary conditions ζ at the western boundary and Neumann boundary conditions at the southern and northern boundaries are applied (Fig. 1). Specifically, at the western boundary the model is forced by a tidal wave with three harmonic constituents (M_2 , M_4 and M_6) with amplitudes $\hat{\zeta}_2$, $\hat{\zeta}_4$ and $\hat{\zeta}_6$; angular frequencies ω , 2ω and 3ω ; and phases ϕ_2 , ϕ_4 and ϕ_6 , which travels from south to north boundaries.

Sediment transport boundary conditions are set by an equilibrium sediment flux, which means sediment flux entering or exiting through the boundaries is nearly perfectly adapted to the local flow conditions and very little accretion or erosion is experienced near the boundaries (Deltares, 2016).

4 Methodology

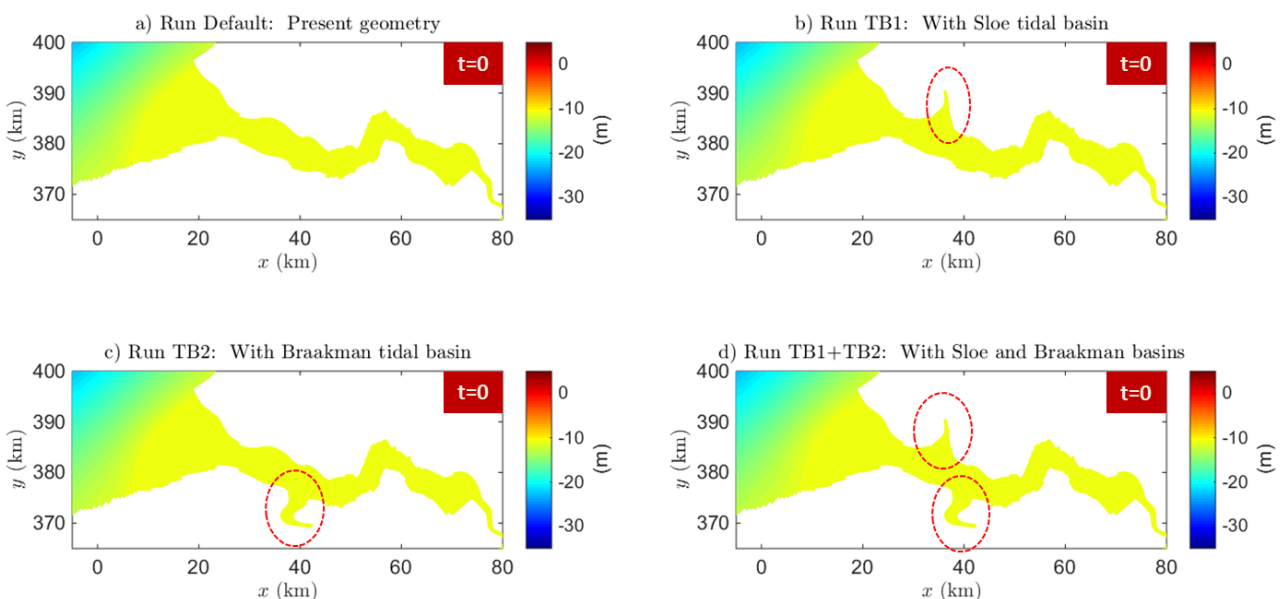
4.1 Experimental set-up

In the default configuration, the present-day geometric shape of Scheldt estuary is considered (Figs. 1 and 6a). A curvilinear grid is created, which extends from Ghent to ~ 30 km seaward. Size of grid cells ranges between 165 m and 500 m in the area of interest (Western Scheldt and its mouth) and it extends to 3 km at offshore boundaries. Runs with 400 year duration are conducted starting from the linear bedlevel profile depicted in Fig. 4 (red line). Non-cohesive sediment is assumed with a single size of 0.2 mm. An erodible layer with a uniform thickness of 50 m is used in the model.

The morphological acceleration factor α_{MOR} is 100, which is often used in morphodynamic studies of estuaries (Canestrelli *et al.*, 2013; Guo *et al.*, 2014; Van der Wegen and Roelvink, 2012). With a hydrodynamic time step Δt of 15 s, the morphodynamic time step is then 25 minutes. Test runs with other values of α_{MOR} show that results are not different. It turns out that even for $\alpha_{\text{MOR}} = 400$, the results are not fundamentally different compared to those for $\alpha_{\text{MOR}} = 100$ (Fig. 15).

Next, three model runs are conducted to quantify effects of secondary tidal basins on the morphodynamic evolution of the estuary and its mouth area. First, in run 'TB1', a tidal basin is constructed on the northern side of the estuary (Fig. 6b) at the same location as that the former basin Sloe (at ~ 22 km from Westkapelle, Fig. 2). Second, in run 'TB2', a tidal basin is added on the southern side of the estuary (Fig. 6c) at same location as that of former basin Braakman (at ~ 30 km from Westkapelle, Fig. 2). Finally, in run 'TB1+TB2', both tidal basins are added to the system (panel d in Fig. 6). Hereafter, the tidal basins described in runs 'TB1', 'TB2' and 'TB1+TB2' are referred to as Sloe, Braakman and Sloe+Braakman basins, respectively.

Figure 6 – Spatial distribution of initial bedlevel z_b (m) in experiments 'Default' (present geometry, panel a), 'TB1' (with Sloe tidal basin, panel b), 'TB2' (with Braakman tidal basin, panel c) and 'TB1+TB2' (with both basins, panel d). Red circles indicate locations of tidal basins.



Finally, sensitivity runs are carried out to investigate sensitivity of model results to effects of river discharge and morphological factor α_{MOR} . An overview of model experiments is presented in Table 1.

Table 1 – List of model runs.

	Name	Description
	<i>Default</i>	Real geometry, width-averaged depth, $\alpha_{MOR} = 100$, $\alpha_{BN} = 2$, $\Delta t = 15$ s
Basins	<i>TB1</i>	With secondary tidal basin Sloe.
	<i>TB2</i>	With secondary tidal basin Braakman.
	<i>TB1+TB2</i>	With both basins Sloe and Braakman.
Other	<i>RiverDis</i>	With river discharge of 50 and 100 m ³ /s.
	<i>Morphac</i>	With morphological factors $\alpha_{MOR} = 100, 200, \text{ and } 300$.

4.2 Methodology to analyze results

A global growth rate σ (yr⁻¹) of bottom patterns is defined, following Garnier *et al.* (2006) and Nnafie *et al.* (2014), as

$$\sigma \equiv \frac{\iint_A h \frac{\partial h}{\partial t} dx dy}{\iint_A h^2 dx dy}, \quad (6)$$

with h the bedlevel change given by $h = z_b(x, y, t) - z_b(x, y, t = 0)$, and A is the surface area (m²). The total simulation time period of model experiments is chosen such that growth rate σ decreases to less than 1% of its initial value σ_0 , with the latter defined as the average value over the first 10 years. Preliminary model runs show that a simulation period of 400 years fulfills the latter condition. Note that although σ becomes small during the simulation period, a perfect morphodynamic equilibrium (i.e., growth rate $\sigma = 0$) is never reached, even for longer time periods.

A comparison is made between present-day measured bedlevel (Fig. 3) and the bedlevel obtained from model experiments after a simulation period of 400 years. Following Van der Wegen and Roelvink (2012) and Guo *et al.* (2014), this comparison focuses on 1) the type and spatial location of large-scale bottom features (shoals and channels), 2) profiles of width-averaged bedlevel ($\langle z_b \rangle$) along the estuary axis, and on 3) hypsometries (i.e., distribution of horizontal surface area A that is located below a certain bedlevel z_b), which provide information about the relative surface area of tidal flats and channels within the domain.

Furthermore, the sand budget of the estuary is analyzed by quantifying its total volume change (V_{tot}) in time, as well as the volume changes over the shoals (V_+) and in the channels (V_-). These quantities are defined as

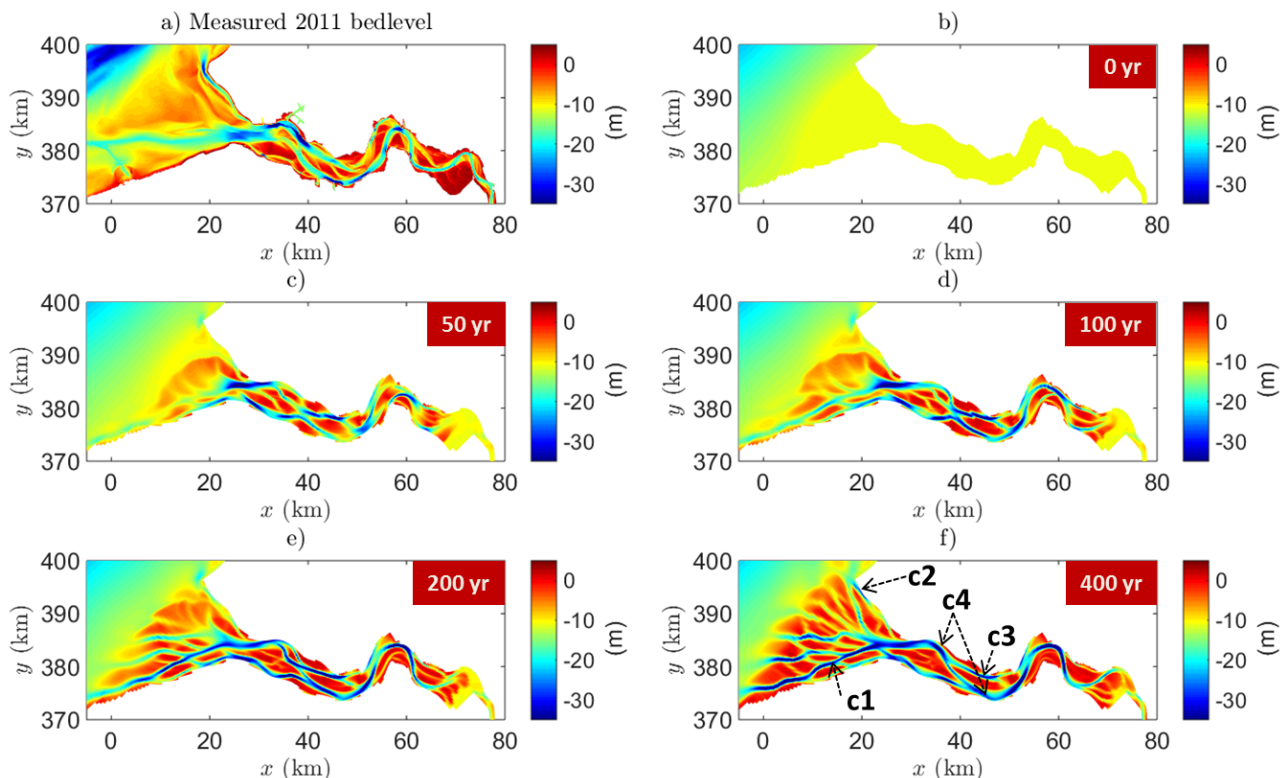
$$\begin{aligned} V_{tot} &= \iint_A h dx dy, \\ V_+ &= \iint_A h dx dy, \quad h \geq 0, \\ V_- &= \iint_A h dx dy, \quad h < 0. \end{aligned} \quad (7)$$

5 Model results

5.1 Default configuration

Figure 7 shows snapshots of bedlevel development in the default configuration after 400 years morphodynamic evolution (panels b-f). By way of comparison, present-day measured bathymetry is also shown (panel a). A relatively fast channel formation (order years to decades, panels b-c) takes place in the narrow transition between estuary and mouth. This channel (*c1*) extends in both seaward and landward directions in the course of time (panels d-f). A large shoal area develops in the mouth (panels c-f), where secondary channels start to occur after ~ 200 years (panels e-f). Another bottom feature that is visible in the mouth area is the formation of a narrow channel (*c2*) along the northern coast of the mouth, which becomes more pronounced with increasing time. In the estuary, a system consisting of straight flood and meandering ebb channels (*c3* and *c4*) forms with large intertidal flats in between. By plotting growth rate σ as a function of time (Fig. 8a), it appears that most morphodynamic activity takes place in the first 50 years. Bedlevel change decreases rapidly with increasing time although morphodynamic activity still continues after 400 years. Fig. 8b compares the modeled bedlevel profile (averaged over the width and applying a 10th order polynomial fit, red line) along the estuary axis with observations (black line). Starting from a linear initial bed (blue line), the simulated bed profile approaches rapidly the measured profile. Overall, the bed profile is characterized

Figure 7 – (b-f) Snapshots of spatial distribution of bedlevel z_b (m) in the $x - y$ domain in the default configuration (run 'Default') at times $t = 0$, $t = 50$, $t = 100$, $t = 200$ and $t = 400$ years. By way of comparison, measured bedlevel is plotted in panel (a). Notations *c1*, *c2*, *c3* and *c4* denote main channels in the region.



by smaller depths in the mouth area and in the upstream part of the Western Scheldt. A larger depth forms at the transition mouth-Western Scheldt, which is caused by strong erosion due to narrowing of width at this location. In the Sea Scheldt, the shallowing of the landward part of the estuary is likely related with the deepening of its seaward part. This means that sand is eroded from the latter part and is deposited in the former part.

Good resemblance between modeled and measured bathymetries is observed, even though also significant differences occur. In particular, the formation of a shallow region in the mouth area flanked by two distinct southern and northern channels ($c1$ and $c2$), and of straight and meandering channels in the estuary ($c3$ and $c4$), are large-scale features that are comparable to present bathymetry. Moreover, the simulated connection between the main ebb channel in the estuary and the southern channel in the mouth, is in agreement with observations. Of particular interest is the continuous extension of channel $c1$ in the offshore direction over time, implying that this process is part of the natural morphodynamic evolution of the system. These results suggest that the observed seaward extension of channel Wielingen between 1800 and 1957 (left panels in Fig. 5) was likely part of the natural evolution of the system towards its morphodynamic equilibrium. On other hand, a significant difference between simulated and measured bathymetries is that channel $c1$ is located too far south in the mouth area compared with the observed main channel (Wielingen). Another major difference is that the simulated shoal area contains many secondary channels compared with observations.

Furthermore, the model simulates a width-averaged bed profile that agrees well with the measured profile. The discrepancy between simulated and measured bed profiles that exists in the landward part of the estuary (Sea Scheldt) is attributed to neglecting river discharge in the simulations. Results from runs 'RiverDis' (Table 1) demonstrate that inclusion of river discharge causes a seaward flushing of sand, thereby reducing sedimentation at the head of the estuary (Fig. 9). Comparison between modeled and measured hypsometries of the estuary (Fig. 10) shows that the distribution of channel and shoal area obtained from the model (blue lines) agree well with observations (black lines). Major differences are that the overall bathymetry produced by the model has a weaker slope, shoals are shallower, and that the main channels ($z_b < -25$ m) are deeper compared with observation (panel a). The overestimation of channel depth by the model occurs particularly in the Western Scheldt (panel c).

Figure 8 – (a) Global growth rate of bedlevel σ (yr^{-1}) versus time. For clarity, a logarithmic scale is used for the y-axis. Dashed black line marks the time at which σ is 1% of σ_0 , with the latter representing average growth rate over the first 10 years. (b) Comparison between measured (black line) and simulated (red line, $t = 400$ years) width-averaged bedlevel (z_b) along the estuary axis for the default run. Initial bedlevel ($t = 0$) is also plotted (dashed blue line). Dashed red lines indicate the different regions of the estuary (mouth, Western Scheldt and Sea Scheldt).

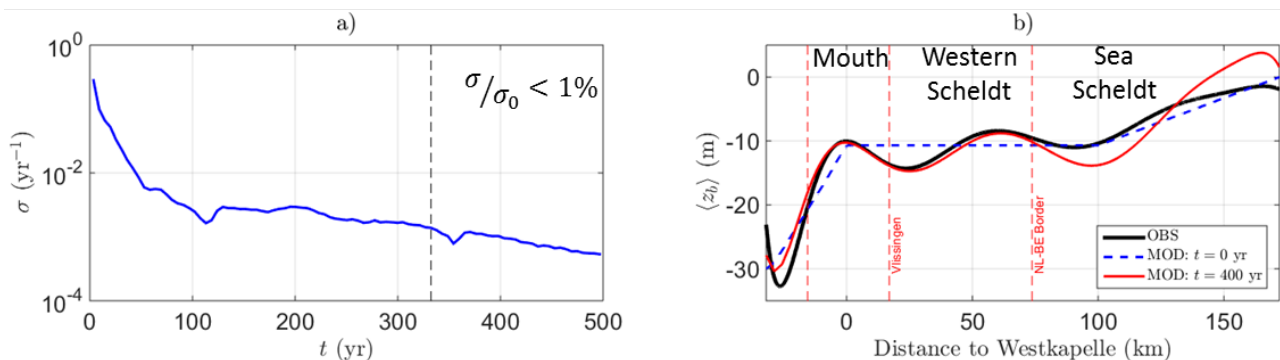


Figure 9 – As in Fig. 8b, but including the cases with river discharge $q = 50 \text{ m}^3/\text{s}$ (green line) and $q = 100 \text{ m}^3/\text{s}$ (magenta line).

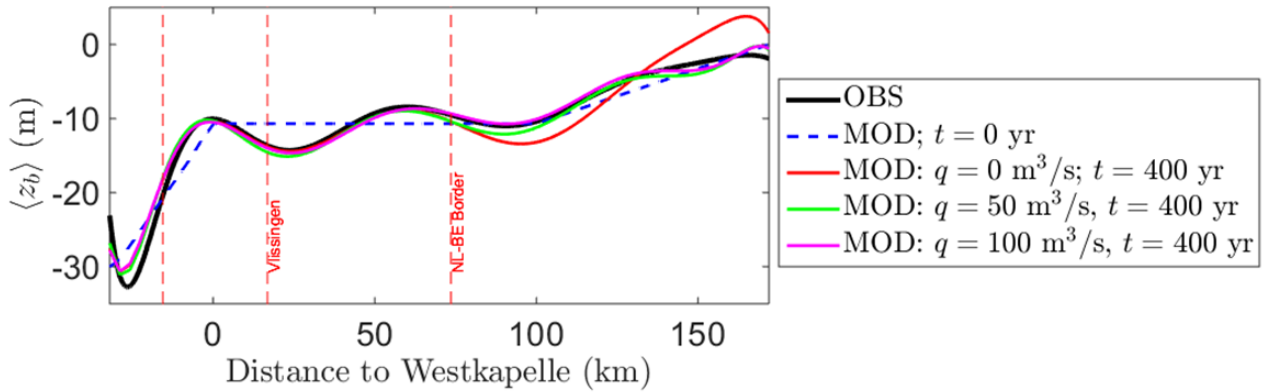
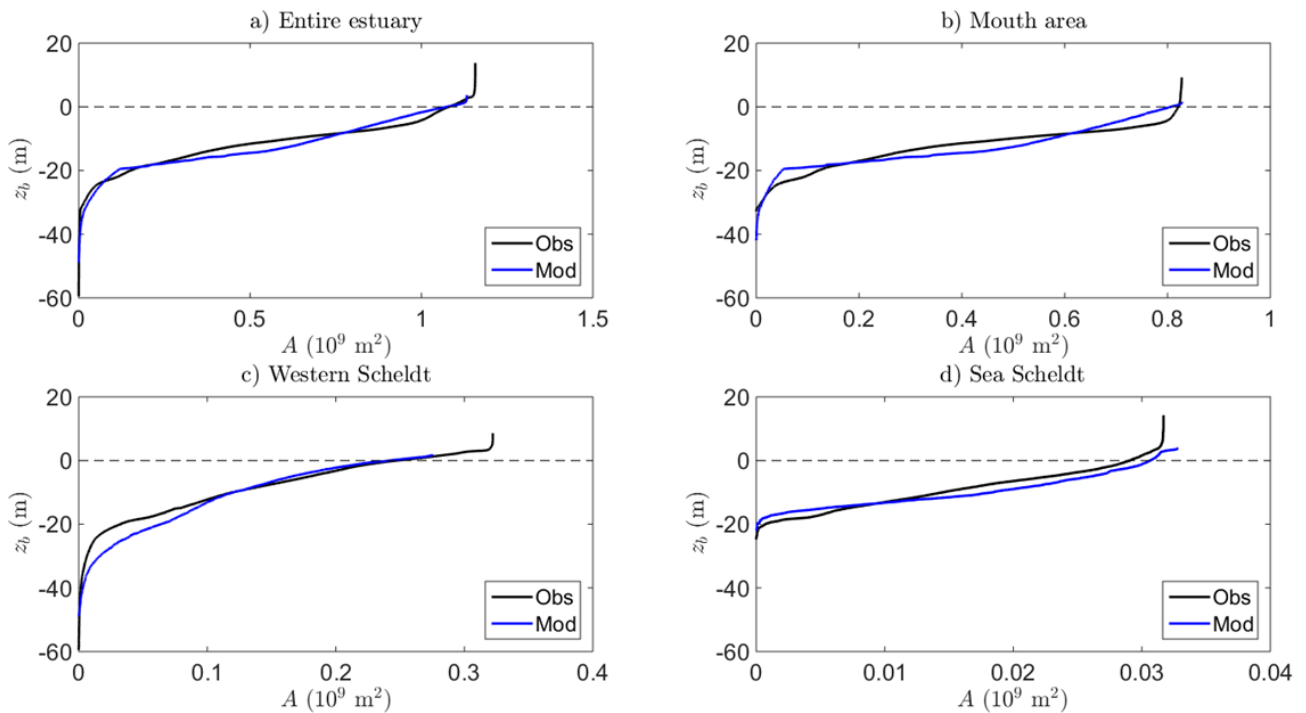


Figure 10 – (a) Comparison between measured (black line) and modeled (blue line) hypsometries (i.e., bathymetric area A located below a specific bedlevel z_b) in the default configuration for the entire area of the estuary. (b-c-d) As in a), but for mouth area (a), Western Scheldt (c) and Sea Scheldt (d). Note that observed bathymetric area A in the Western Scheldt is larger than that in the model due to the fact that the model grid does not cover same parts of the Western Scheldt area, such as the Sloe Harbor near Vlissingen (see Fig. 1).



With regard to sand balance of the study area, results (Fig. 11a) reveal that the estuary (excluding its mouth, black line) experiences a yearly-averaged sand loss of $\sim 0.3 \times 10^6 \text{ m}^3$ per year, which is deposited in the mouth area (blue line). Besides sand that comes from the estuary, additional sand is transported from elsewhere in the North Sea into the mouth area (result not shown), resulting in a yearly averaged accretion of $\sim 1 \times 10^6 \text{ m}^3/\text{yr}$. Moreover, from Fig. 11 (panels b, c and d), it appears that sand needed for development of shoals (ΔV_+ , dashed lines) and channels (ΔV_- , dotted lines) is provided mainly through local redistribution of sand. Including river discharge (Fig. 12) causes a net sand gain in the landward part of the estuary (Sea Scheldt, green lines) and it slightly reduces the

sand export to the mouth area (blue lines).

5.2 Effects of secondary tidal basins

Results in case of secondary tidal basin Sloe (experiment 'TB1', Fig. 13b) reveal that the seaward part of ebb channel $c4$ forms about 2 km southward with respect to that in case of no tidal basin (panel a). This implies that the presence of this basin causes a locally southward migration of the ebb channel. Moreover, these results show that the presence of this basin causes a more seaward extension of flood channel $c3$ compared to that in the default case. In case of Braakman tidal basin (experiment 'TB2', panel c), the connection between the landward and seaward parts of the ebb channel weakens, which results in a decrease of the sinuosity (meander) of this channel. The presence of Braakman basin does not result in a local displacement of the ebb channel, which reveals the importance of

Figure 11 – (a) Time evolution of the cumulative sand volume change ΔV_{tot} (10^9 m^3) for the different sections of the estuary (Western Scheldt and Sea Scheldt) and its mouth area in the default experiment. (b) Time evolution of the relative contributions to total cumulative sand volume change (ΔV_{tot}) of volume changes caused by shoal and channel formation in the mouth area (ΔV_+ and ΔV_- , respectively). (c-d) As in (b), but for Western Scheldt (c) and Sea Scheldt (d).

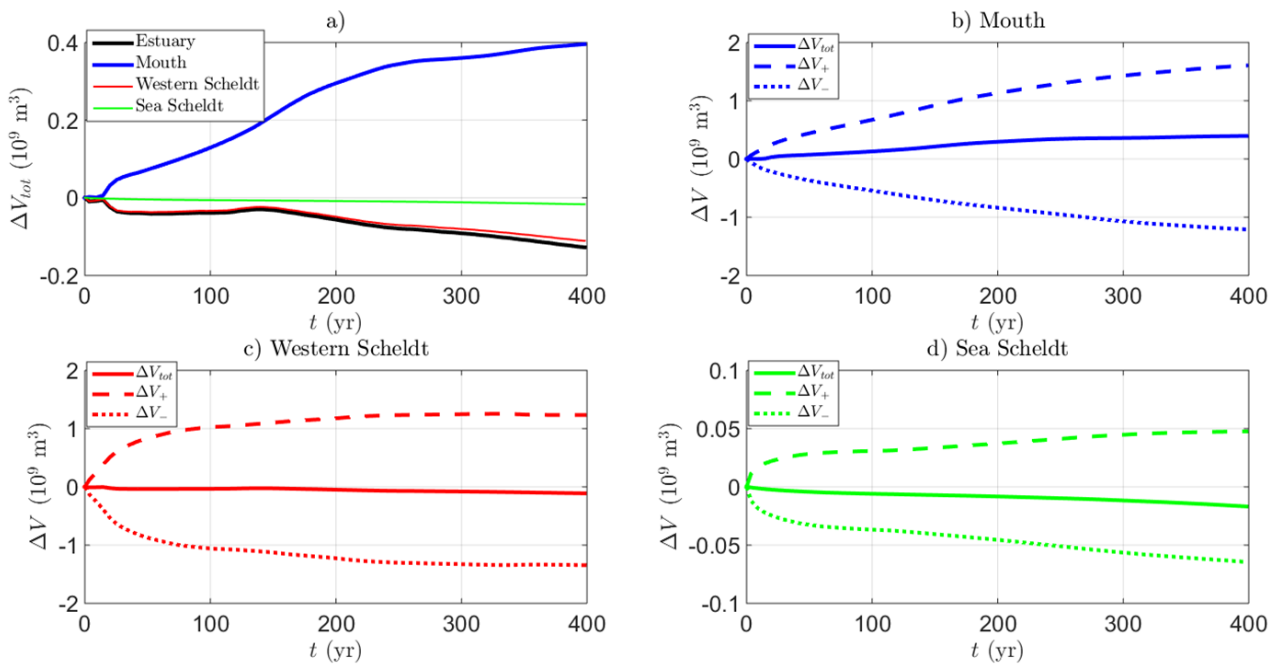
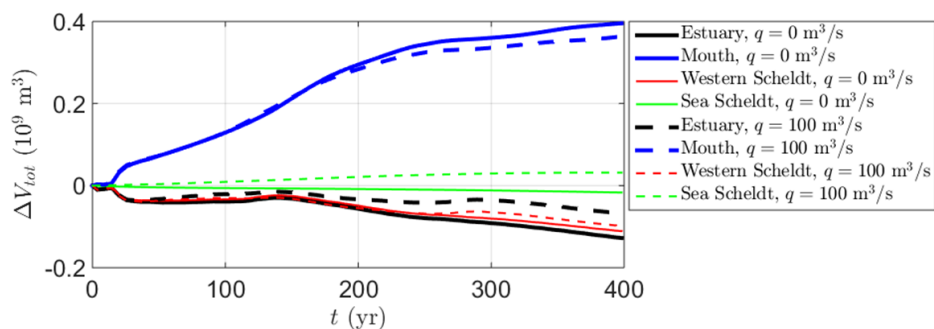


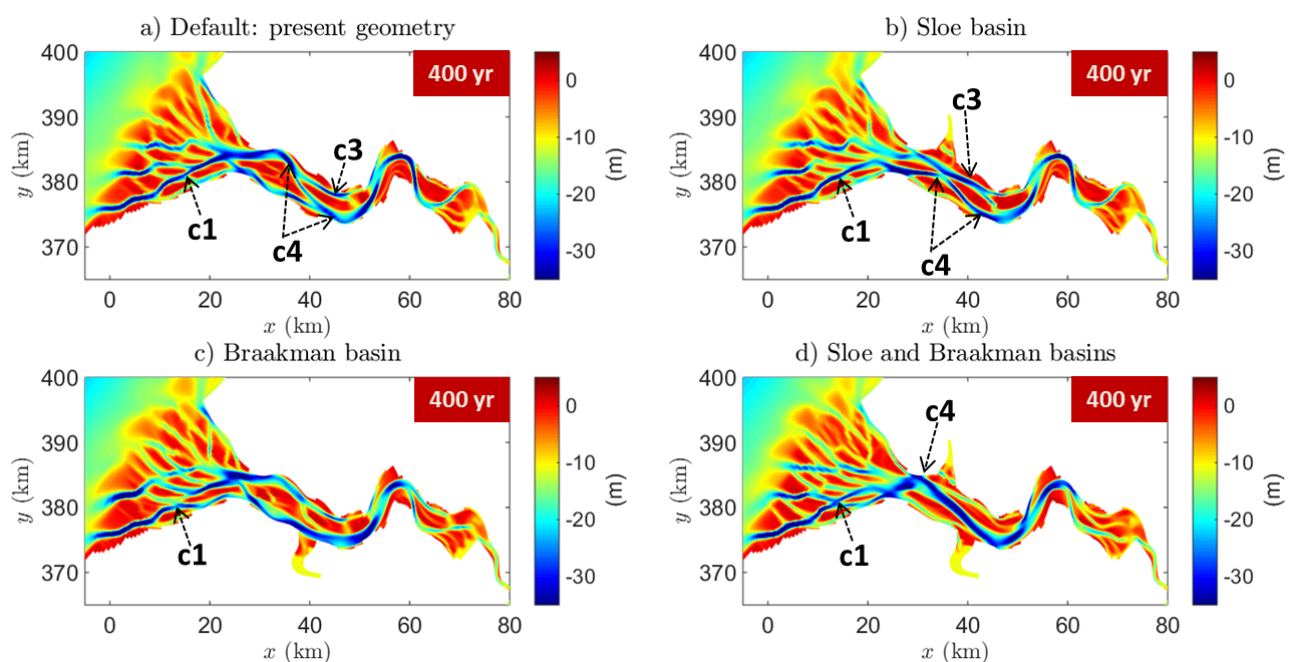
Figure 12 – As in Fig.11a, but including the case with a river discharge of $100 \text{ m}^3/\text{s}$ (dashed lines, run 'RiverDis' in Table 1).



basin location. Similar to experiment 'TB1', in case of adding two secondary basins (Sloe+Braakman, panel d) a southward shift of the ebb channel near the location of Sloe basin appears. Note that in the latter case the channel curve is located seaward of the Sloe basin. Moreover, formation of straight flood channels are less visible in the case of Sloe+Braakman basins. The locally southward displacements of the main ebb channel near the Sloe basin provides support for the hypothesis that observed northward shift of Honte is caused by closure of this basin. Fig. 13 further shows that presence of secondary tidal basins in the estuary leads to changes in the shape of meandering ebb channel (*c4*), such that the connection between the latter channel and the southern channel in the mouth area (*c1*) is weakened, particularly in the case of Braakman basin (panel c). This means that the presence of a secondary tidal basin inside the estuary not only have local morphodynamic effects, but it can also have significant effects on the morphodynamic evolution of the mouth of the estuary.

Regarding changes in sand balance of the system, from Fig. 14a it is seen that the presence of Sloe basin changes the sand balance of particularly the Western Scheldt (dashed red line) and the mouth (dashed blue line). Compared with the case of no basin (solid lines in this figure), the sand export from the estuary to its mouth is reduced by a yearly averaged amount of $\sim 0.25 \times 10^6 \text{ m}^3/\text{yr}$. Of particular interest is the alternating periods of sand import to and export from the estuary that occurs within the simulation time period. In the first 100 years, hardly any sand is lost in the estuary. Subsequently, between $t \approx 100 \text{ yr}$ and $t \approx 170 \text{ yr}$, sand is imported into the estuary at a yearly averaged rate of $\sim 0.9 \times 10^6 \text{ m}^3/\text{yr}$. Next, for $t > 170 \text{ yr}$, the estuary experiences a sand loss of $\sim 0.25 \times 10^6 \text{ m}^3/\text{yr}$. Compared with the default case (no secondary basin), adding the Braakman basin to the system causes no significant changes in the sand balance of the estuary and its mouth during the initial time period ($t < 170 \text{ yr}$, dashed lines in Fig. 14b). In the subsequent period, however, sand import takes place from the mouth to the estuary between $t = 170 \text{ yr}$ and $t = 280 \text{ yr}$ ($\sim 0.3 \times 10^6 \text{ m}^3/\text{yr}$), followed by a period of sand export ($\sim 0.3 \times 10^6 \text{ m}^3/\text{yr}$) to the mouth. Note that sand that comes from the North Sea into the mouth area reduces after $t > 170 \text{ yr}$ (result not shown). Adding two secondary basins (Sloe+Braakman) to the system changes the sand balance even more compared with the cases of adding one basin only (Fig. 14c, dashed lines). Periods of sand import ($\sim 0.5 \times 10^6 \text{ m}^3/\text{yr}$) followed

Figure 13 – Snapshots of spatial distribution of bedlevels after 400 years in the default case (a), in the cases of including either Sloe (b) or Braakman (c) tidal basins, and in the case of including both basins (d).



by sand export ($\sim 0.7 \times 10^6 \text{ m}^3/\text{yr}$) characterize the sand balance of the estuary. Also, sand coming from elsewhere in the North Sea to mouth area decreases significantly. As a result, the net sand gain in the mouth area reduces by a yearly averaged amount of $\sim 0.65 \times 10^6 \text{ m}^3/\text{yr}$. Note that the sand balance of the landward part of the estuary (Sea Scheldt) is hardly affected by the presence of secondary tidal basins (green lines in Fig. 14). The changes in the sand balance occur mainly in the Western Scheldt (red lines) and its mouth area (blue lines).

Figure 14 – As in Fig.11a, but in cases of including Sloe basin (a), Braakman basin (b), and both Sloe and Braakman basins (c). In each panel, solid and dashed lines indicate the cases without and with a secondary basin, respectively.

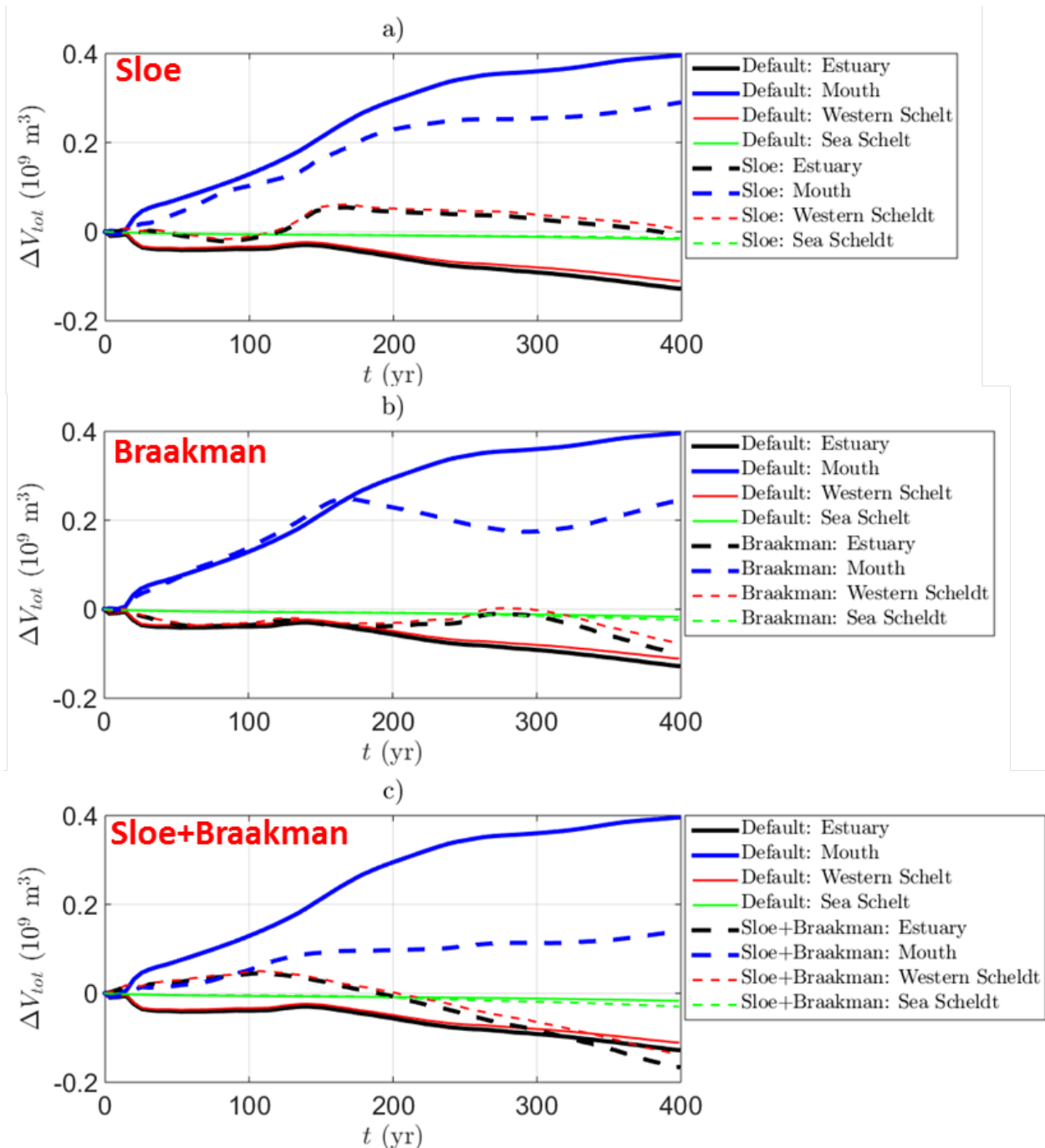
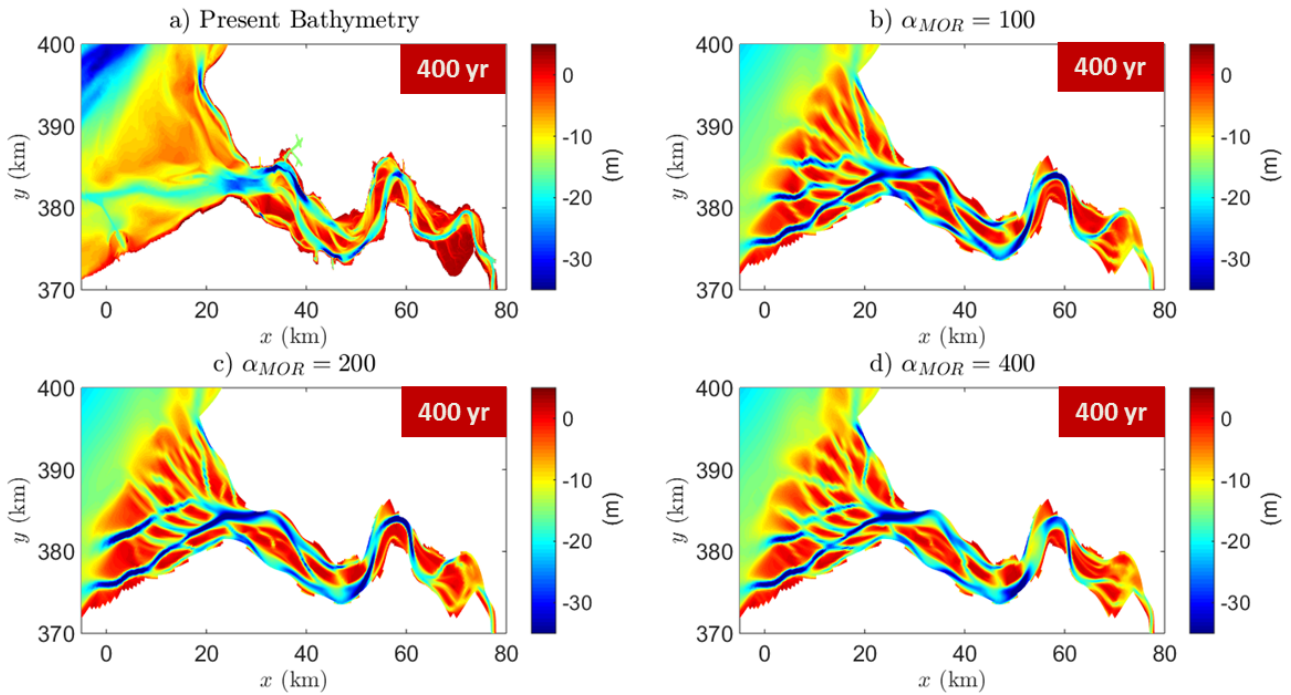


Figure 15 – Spatial distribution of bedlevel in case of morphological amplification factors $\alpha_{MOR} = 100$ (b), $\alpha_{MOR} = 200$ (c) and $\alpha_{MOR} = 400$ (d) (experiment 'Morphac' in Table 1). Panel a) shows measured bedlevel.



5.3 Sensitivity to morphological factor

Fig. 15 shows that results for morphological factors up to 400 do not significantly differ from each other. Formation of southern and northern channels in the mouth area, and a system of straight flood and meandering ebb channels is obtained in all the cases. However, a factor of 100 is used in this study to guarantee the optimal accuracy of model results versus a fast model running time.

6 Discussion and Conclusions

The specific objective of this study was to investigate the impact of the presence of secondary tidal basins on long-term estuarine morphodynamics. To this end, first, a morphodynamic model using Delft3D is developed, which is able to reproduce large-scale bottom features similar to those observed in a real estuary. Second, runs are conducted with the latter model in case that secondary tidal basins are present. The study area is the Scheldt estuary because it used to consist of multiple secondary tidal basins that were gradually closed off over the last two centuries. The large availability of historical data on its geometry and bathymetry since 1800 offers a great opportunity to compare model results with observations.

Good resemblance between modeled and measured bathymetry is observed, even though also significant differences occur. In particular, the formation of a shallow region in the mouth area flanked by two distinct southern and northern channels, and of a system of straight and meandering channels in the estuary, are large-scale features that are comparable to present bathymetry. Moreover, the simulated connection between the main ebb channel in the estuary and the southern channel in the mouth is in agreement with observations. The continuous extension of southern channel in the offshore direction with increasing time implies that this process is part of the natural morphodynamic evolution of the system. This suggests that the observed seaward extension of channel Wielingen between 1800 and 1957 was likely part of the natural evolution of the system towards its morphodynamic equilibrium. On the other hand, a significant difference between simulated and measured bathymetries, is that the southern channel in the mouth area forms too far south compared with observed main channel (Wielingen). Another major difference is that the simulated shoal area contains many secondary channels compared with observations, which is attributed to neglecting of waves. Eelkema *et al.*, 2013 pointed out that inclusion of waves particularly leads to a redistribution of sediment from shoals into channels. Results from preliminary model runs show that by accounting for waves, the secondary channels disappear in the mouth area (Fig. 16). However, the used wave forcing in these runs is highly simplified by assuming that this forcing remains constant in time at the offshore boundaries, and that waves come from one direction. Further research still needs to be carried out to properly account for effects of variations in wave height and direction on estuarine morphodynamics. Furthermore, model simulates a width-averaged bed profile that agrees well with the measured profile, particularly in the case of accounting for river discharge. Comparison between modeled and measured hypsometries of the estuary shows that the distributions of channel and shoal area obtained from the model agree well with observations. Major differences are that the overall bathymetry produced by the model has a weaker slope, shoals are shallower, and that the main channels are deeper compared with observations.

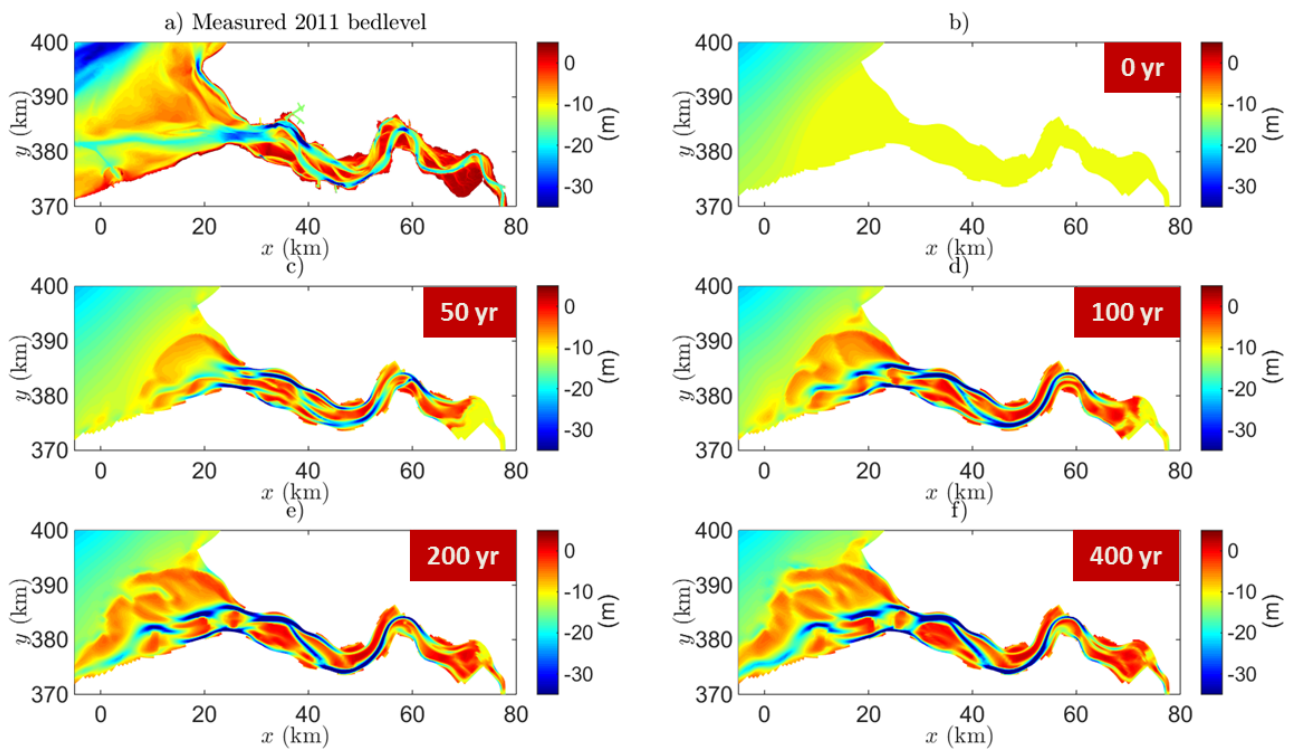
In case that a secondary tidal basin is constructed on the northern side of the estuary (Sloe basin), the seaward part of the main ebb channel shifts about 2 km southward with respect to location of this basin. Similar shift is observed in case that two secondary tidal basins are added to the estuary (Sloe and Braakman basins). These results provide support for the hypothesis that the observed northward shift of seaward part of the main ebb channel (Honte) is caused by closure of former tidal basin Sloe. In case of adding a secondary tidal basin on the southern side of the estuary (Braakman), a system of straight flood and meandering ebb channels in this case is less clear compared with the default case and the cases of Sloe+Braakman and Sloe. Results further reveal that the presence of secondary tidal basins in the estuary weakens connection between the main ebb channel in the estuary and the southern channel in the mouth area, particularly in the case of Braakman tidal basin.

With regard to estuarine sand balance, model results show that the estuary with its present-day geometric shape experiences a yearly averaged sand loss of $\sim 0.3 \times 10^6 \text{ m}^3/\text{yr}$, which is deposited in the mouth area. The presence of secondary tidal basins has a significant impact on the sand balance of particularly the seaward part of the estuary (Western Scheldt) and its mouth area. Of particular interest is the occurrence of alternating periods of sand import and export in the estuary within the simulation time period in case that a secondary tidal basin is added to the system. In the case that such a basin is added north of the estuary (Sloe), hardly any sand is lost from the estuary in the first 100 years. Next, the estuary experiences a period of sand import of $\sim 0.9 \times 10^6 \text{ m}^3/\text{yr}$ followed by sand export of $\sim 0.25 \times 10^6 \text{ m}^3/\text{yr}$ to mouth area. Compared with the default case (no secondary basin), adding the Braakman basin to the system causes no significant changes in the sand balance of the estuary and its mouth during the initial time period, meaning that the estuary keeps also losing sand in this case. In the subsequent period, however, a period of sand import of $\sim 0.3 \times 10^6 \text{ m}^3/\text{yr}$ followed by a period of export of $\sim 0.3 \times 10^6 \text{ m}^3/\text{yr}$ take place in the estuary. Adding two secondary basins (Sloe+Braakman) to the system changes the sand balance even more compared with the cases of adding one basin only. Periods of sand import ($\sim 0.5 \times 10^6 \text{ m}^3/\text{yr}$) followed by sand export ($\sim 0.7 \times 10^6 \text{ m}^3/\text{yr}$) characterizes the sand balance of the estuary. Furthermore, the presence of secondary tidal basins significantly reduces sand coming from other parts of the sea to the mouth area, particularly in the case Sloe+Braakman.

The study by Haring (1955) showed that during the period 1878-1952, the Western Scheldt was a sand importing system (yearly averaged import of $\sim 1.3 \times 10^6 \text{ m}^3/\text{yr}$). Since 1952, alternating periods of sand import and export took place (Kuijper *et al.*, 2004). Recent studies on sand balance in the Western Scheldt (IMDC, 2013; Taal *et al.*, 2013) concluded that the latter area loses sand to the mouth. Based on the model results, it is likely that the observed changes in the sand balance of the estuary are partly caused by closure of former tidal basins Sloe and Braakman. However, comparison between model results and observations is not straightforward, because other factors such as dredging and dumping activities and the 18.6 year nodal cycle (not present in the model) can significantly influence the sand balance of the estuary (Jeuken *et al.*, 2003; Kuijper *et al.*, 2004). Moreover, the closure of former basins Sloe and Braakman took place gradually between 1800 and 1968 (Van der Spek, 1997).

In conclusion, in the case of using present-day geometric shape of the Scheldt estuary, the observed large-scale bottom features in this estuary are reproduced well by the model. In particular, the formation of a shallow region in the mouth of the estuary flanked by two distinct southern and northern channels, and of a system of straight and meandering channels inside the estuary, are large-scale features that are comparable to observed bathymetry. The presence of secondary tidal basins as well as their location within the estuary have a significant impact particularly on the shape of the meandering main channel in the estuary. Namely, depending on the location of the basin within the estuary, the latter channel forms more to the south compared to its position in case of no basin. The changes in the shape of the meandering channel are such that its connection with the southern channel in the mouth area is weakened. This means that the presence of a secondary tidal basin inside the estuary not only have local morphodynamic effects, but it can also have significant effects on the morphodynamic evolution of other areas, such as the mouth of the estuary. Furthermore, the presence of secondary basins significantly influences sand balance of the estuary, even on longer time scales (in the order of centuries). Model results confirm the hypothesis that the observed northward migration of the ebb channel near the location of the former secondary basin Sloe is due to closure of this basin. Moreover, these results suggest that the observed widening and seaward extension of channel Wielingen over the last two centuries were part of the natural evolution of the system towards its morphodynamic equilibrium. However, the closure of the Sloe and Braakman basin might probably have contributed to the observed changes in Wielingen.

Figure 16 – As in Fig. 7, but in the case that waves are accounted for.



References

- Alebregtse, N.; Swart, H. de** (2014). Effect of a secondary channel on the non-linear tidal dynamics in a semi-enclosed channel: a simple model. *Ocean dynamics* 64 (4): 573–585
- Bolle, A.; Wang, Z. B.; Amos, C.; De Ronde, J.** (2010). The influence of changes in tidal asymmetry on residual sediment transport in the Western Scheldt. *Continental Shelf Research* 30 (8): 871–882
- Brand, E.; Van Oyen, T.; Van der Vegt, M.** (2016). The driving mechanisms behind morphological changes in the Western Scheldt mouth area over the past two centuries – a data analysis. *techreport*. Final report of MSc. thesis, Utrecht University (The Netherlands) and Flanders Hydraulics Research (Belgium)
- Canestrelli, A.; Lanzoni, S.; Fagherazzi, S.** (2013). One-dimensional numerical modeling of the long-term morphodynamic evolution of a tidally-dominated estuary: The lower Fly River (Papua New Guinea). *Sediment. Geol.* 301: 107–119
- Dam, G.; Wegen, M.; Labeur, R.; Roelvink, D.** (2016). Modeling centuries of estuarine morphodynamics in the Western Scheldt estuary. *Geophysical Research Letters*
- Deltares Delft, T. N.** (2016). User manual Delft3D-Flow: Simulation of multi-dimensional hydrodynamic flows and transport phenomena, including sediments. *techreport*
- Dissanayake, D.; Ranasinghe, R.; Roelvink, J.** (2012). The morphological response of large tidal inlet/basin systems to relative sea level rise. *Climatic change* 113 (2): 253–276
- Du Four, I.; Schelfaut, K.; Vanheteren, S.; Van Dijk, T.; Van Lancker, V.** (2006). Geologie en sedimentologie van het Westerscheldemondingsgebied. *Coosen J., Mees J., Seys J. en Fockedey N.(Eds.). Studiedag: De Vlakte van de Raan van onder het stof gehaald. Oostende 13*
- Eelkema, M.; Wang, Z. B.; Hibma, A.; Stive, M. J.** (2013). Morphological effects of the Eastern Scheldt storm surge barrier on the ebb-tidal delta. *Coastal Engineering Journal* 55 (03): 1350010
- Enckevort, I. van** (1996). Morfologisch onderzoek Westerschelde monding. Deel 2: Morfologische ontwikkeling van de Westerschelde monding sinds 1800. *techreport*. IMAU, Utrecht University
- Engelund, E.; Hansen, E.** (1967). A monograph on sediment transport in alluvial streams. *techreport*. Teknisk Forlag: Copenhagen, Denmark
- Flokstra, C.; Koch, F.** (1981). Numerical aspects of bed level predictions for alluvial river bends. *Delft Hydraulics Laboratory. Netherlands, Publication (258)*
- Garnier, R.; Calvete, D.; Falqués, A.; Caballeria, M.** (2006). Generation and nonlinear evolution of shore-oblique/transverse sand bars. *Journal of Fluid Mechanics* 567: 327–360
- Guo, L.; Wegen, M.; Roelvink, J.; He, Q.** (2014). The role of river flow and tidal asymmetry on 1-D estuarine morphodynamics. *Journal of Geophysical Research: Earth Surface* 119 (11): 2315–2334
- Haring, J.** (1955). Inhouds- en diepteveranderingen Westerschelde 1931–1952. *techreport*. Directie Benedenrivieren, Studiedienst, Report D164 (in Dutch)

- Hibma, A.; Schuttelaars, H. M.; Wang, Z. B.** (2003). Comparison of longitudinal equilibrium profiles of estuaries in idealized and process-based models. *Ocean Dynamics* 53 (3): 252–269
- IMDC, D. S.** (2013). Grootchalige sedimentbalans van de Westerschelde. *techreport*. Basisrapport grootchalige ontwikkeling G-2, IMDC
- Jeuken, M.; Wang, Z.** (2010). Impact of dredging and dumping on the stability of ebb–flood channel systems. *Coastal Engineering* 57 (6): 553–566
- Jeuken, M.; Wang, Z.; Keillerc, D.; Townend, I.; Lieke, G.** (2003). Morphological response of estuaries to nodal tide variation
- Kuijper, C.; Steijn, R.; Roelvink, J.; Kaaij, T.; Olijslagers, P.** (2004). Morphological modelling of the Western Scheldt: validation of DELFT3D. *techreport*. Deltares (WL)
- Kuijper, K.; Lescinski, J.** (2012). Data analyses and hypotheses Western Scheldt. *techreport*. Deltares, The Netherlands. Project number 1204405. 187p
- Lesser, G.; Roelvink, J.; Van Kester, J.; Stelling, G.** (2004). Development and validation of a three-dimensional morphological model. *Coastal engineering* 51 (8): 883–915
- Nnafie, A.; Swart, H. E. de; Garnier, R.; Calvete, D.** (2014). Modeling the response of shoreface-connected sand ridges to sand extraction on an inner shelf. *Ocean Dynamics* 53: 1–18. DOI: 10.1007/s10236-014-0714-9
- Peters, J. J.** (2006). Belang van de Vlakte van de Raan voor de morfologische evoluties van het Schelde-estuarium. *Studiedag: De Vlakte van de Raan van onder het stof gehaald*. *Oostende* 13: 30–42
- Peters, J.; Meade, R.; Parker, W.; Stevens, M.** (2001). Improving navigation conditions in the Westerschelde and managing its estuarine environment. *How to harmonize accessibility, safety and naturalness*
- Ridderinkhof, W.; Swart, H. E. de; Vegt, M. van der; Hoekstra, P.** (2014). Influence of the back-barrier basin length on the geometry of ebb-tidal deltas. *Ocean Dynamics* 64: 1333–1348. DOI: 10.1007/s10236-014-0744-3
- Roelvink, J.** (2006). Coastal morphodynamic evolution techniques. *Coastal Engineering* 53 (2): 277–287
- Roos, P. C.; Schuttelaars, H. M.** (2015). Resonance properties of tidal channels with multiple retention basins: role of adjacent sea. *Ocean dynamics* 65 (3): 311–324
- Slikke M. J., V. der** (1999). Morfologische ontwikkeling Westerscheldemonding tot 2020, een fenomenologische visie. *techreport*. Institute for Marine and Atmospheric Research Utrecht (IMAU), Utrecht University, The Netherlands
- Spek, A. J. F. van der** (1994). Large-scale evolution of Holocene tidal basins in the Netherlands. Universiteit Utrecht, Faculteit Aardwetenschappen
- Taal, M.; Wang, Z.; Cleveringa, J.** (2013). LTV Veiligheid en Toegankelijkheid.G-13:Synthese en conceptueel model. *techreport*. Basisrapport grootchalige ontwikkeling. Deltares
- Van den Berg, J.** (1987). Toelichting bij de isallobatenkaart Voordelta 1975 - 1984. *techreport*. Rijkswaterstaat Report, ZL 87.0020

Van der Spek, A. (1997). Tidal asymmetry and long-term evolution of Holocene tidal basins in The Netherlands: simulation of palaeo-tides in the Schelde estuary. *Marine Geology* 141 (1): 71–90

Van der Wegen, M.; Roelvink, J. (2008). Long-term morphodynamic evolution of a tidal embayment using a two-dimensional, process-based model. *Journal of Geophysical Research: Oceans* 113 (C3)

Van der Wegen, M.; Roelvink, J. (2012). Reproduction of estuarine bathymetry by means of a process-based model: Western Scheldt case study, the Netherlands. *Geomorphology* 179: 152–167

Van Oyen, T.; Van der Vegt, M.; De Maerschalk, B.; Nnafie, A.; Verwaest, T.; Mostaert, F. (2016). Verbetering Modelinstrumentarium Lange termijn Morfologie. *techreport*. Flanders Hydraulics Research, Antwerp, Belgium

Van Rijn, L. (2010). Tidal phenomena in the Scheldt Estuary. *Report, Deltares*

Wang, Z.; Jeuken, M.; Gerritsen, H.; De Vriend, H.; Kornman, B. (2002). Morphology and asymmetry of the vertical tide in the Westerschelde estuary. *Continental Shelf Research* 22 (17): 2599–2609

Wang, Z.; Ronde, J. de; Spek, A. van der; Elias, E. (2009). Response of the Dutch coastal system to (semi-) closures of tidal basins. *in: Proceedings of ICEC 2009, Sendai, Japan*. Vol. 1. pp. 203–210

Winterwerp, J.; Wang, Z.; Stive, M.; Arends, A.; Jeuken, C.; Kuijper, C.; Thoolen, P. (2001). A new morphological schematization of the Western Scheldt estuary, The Netherlands. *in: Proceedings of the 2nd IAHR symposium on River, Coastal and Estuarine Morphodynamics*. pp. 525–533

Winterwerp, J. C.; Wang, Z. B. (2013). Man-induced regime shifts in small estuaries—I: theory. *Ocean Dynamics* 63 (11-12): 1279–1292

DEPARTMENT **MOBILITY & PUBLIC WORKS**
Flanders hydraulics Research

Berchemlei 115, 2140 Antwerp

T +32 (0)3 224 60 35

F +32 (0)3 224 60 36

waterbouwkundiglabo@vlaanderen.be

www.flandershydraulicsresearch.be